

Multicritical behaviour in the q-state Potts lattice-gas

This article has been downloaded from IOPscience. Please scroll down to see the full text article.

1984 J. Phys. A: Math. Gen. 17 1703

(<http://iopscience.iop.org/0305-4470/17/8/025>)

View [the table of contents for this issue](#), or go to the [journal homepage](#) for more

Download details:

IP Address: 129.252.86.83

The article was downloaded on 31/05/2010 at 08:36

Please note that [terms and conditions apply](#).

Multicritical behaviour in the q -state Potts lattice-gas

T Temesvári† and L Herényi‡

† Institute for Theoretical Physics, Eötvös University, H-1088 Budapest, Puskin u. 5-7, Hungary

‡ Biophysical Research Laboratory of Hungarian Academy of Sciences, H-1088 Budapest, Puskin u. 9, Hungary

Received 12 October 1983

Abstract. The phase diagram of the q -state Potts lattice-gas (or site-diluted Potts model) is studied in this paper. After listing some rather simple results for different limiting cases of the interaction parameters, an exact mapping between the two-state model, which is equivalent to the Blume–Emery–Griffiths model, subjected to a special constraint and the pure Ising model is given for lattices with coordination number three. Thus, an exact intersection of the critical surface is obtained on the honeycomb lattice. The model has a complex phase diagram on the Cayley tree (or Bethe lattice): two types of critical endpoints, tricritical points and a tetracritical point are located for $1 \leq q < 2$. The nature of the phase transition at multicritical points changes abruptly at $q = 2$. We argue that the tetracritical point might be found also in lower dimensions if q is less than some $q_m(d)$. The three-dimensional Blume–Emery–Griffiths and correlated site–bond percolational models are the important cases conjectured to have tetracritical points. The divergence of the susceptibility in spite of the discontinuity of the order parameter at the pure $(q+1)$ -state Potts transition point is found on the Cayley tree ($1 < q < 2$). This phenomenon, which is due to the fact that the line of tricritical points terminates at the $(q+1)$ -state Potts transition point, might also be present in lower dimensions in accordance with series expansion and Monte Carlo results.

1. Introduction

In this paper we study a model with magnetic and non-magnetic atoms (spins and vacancies) in thermal equilibrium, where the spins can take one of q equivalent states. When the density of vacancies vanishes, it reduces to the pure q -state Potts (1952) model which has been the subject of intensive studies in recent years. In this system there is a single second-order phase transition which turns to first order at $q = q_c(d)$, where q_c depends only on the dimension of the lattice (Wu 1982). The failure of position–space renormalisation-group methods to detect this changeover in the character of the phase transition suggested the introduction of vacancies into the system, thus enlarging the parameter space so that the pure model was mapped onto a diluted one under renormalisation (Nienhuis *et al* 1979). Three fixed points were obtained: a critical one governing the surface of second-order phase transitions which also contained the pure model critical point; a discontinuity fixed point for first-order transitions and a tricritical one separating the two different ranges of the phase boundary. At q_c the critical and tricritical fixed points merged and the whole phase boundary became governed by the discontinuity fixed point. This mechanism was first

found in the 2D case where $q_c = 4$ is known exactly (Baxter 1973). More elaborate works obtained good agreement with this value (Nienhuis *et al* 1980a, Burkhardt 1980).

The model can be defined by the Hamiltonian

$$\mathcal{H} = -J \sum_{\langle ij \rangle} [(\delta_{s_i, s_j} - 1)t_i t_j + \alpha t_i t_j] + \sum_i [\mu - h(\delta_{s_i, 1} - 1)]t_i, \quad (1)$$

where $t_i = 0$ ($t_i = 1$) if the lattice site i is vacant (occupied) and s_i assumes one of the values $1, 2, \dots, q$ if $t_i = 1$. The Potts interaction is given by the Kronecker delta, while the parameter α characterises the lattice-gas coupling. The density of magnetic atoms is governed by the chemical potential μ , and the last term in (1) breaks the symmetry of the Potts spins preferring the state 1 for a positive magnetic field. Only nearest-neighbour ferromagnetic interactions ($J, \alpha \geq 0$) will be considered.

For some special values of q the diluted q -state Potts model (or Potts lattice-gas) defined by (1) has been investigated intensively for many years. The $q = 2$ case, which has been studied longest, is exactly the three-component or $S = 1$ Ising model, first proposed to describe the first-order transition found in magnetic systems consisting of triplet ions ($S = 1$) with zero-field splitting (Blume 1966, Capel 1966). Its extended version containing a coupling between the singlet ($S_z = 0$) and doublet ($S_z = \pm 1$) states was later applied to ^3He - ^4He mixtures where first-order phase separation between the two species or second-order superfluid transition takes place depending on the density of ^3He atoms (Blume *et al* 1971). Some other applications to systems having tricritical phase diagrams were also proposed (Lajzerowicz and Sivardière 1975, Sivardière and Lajzerowicz 1975a, b). It is worthwhile writing down the form of the Hamiltonian used in these references:

$$\tilde{\mathcal{H}} = - \sum_{\langle ij \rangle} (\tilde{J}\tilde{S}_i\tilde{S}_j + \tilde{K}\tilde{S}_i^2\tilde{S}_j^2) + \sum_i (\tilde{\Delta}\tilde{S}_i^2 - \tilde{H}\tilde{S}_i), \quad (2)$$

where $\tilde{S}_i = 0, \pm 1$. The following equations ensure that the two-state Potts lattice-gas and the model defined by equation (2), which we will refer to as the Blume-Emery-Griffiths model (BEG), are equivalent

$$\mu = \tilde{\Delta} - \tilde{H}, \quad h = 2\tilde{H}, \quad J = 2\tilde{J} \quad \text{and} \quad \alpha = \frac{1}{2}(1 + \tilde{K}/\tilde{J}). \quad (3)$$

The BEG system has been investigated so far by several forms of the mean-field theory (Blume 1966, Capel 1966, Blume and Watson 1967, Blume *et al* 1971, Mukamel and Blume 1974, Lajzerowicz and Sivardière 1975, Sivardière and Lajzerowicz 1975a, b, Furman *et al* 1977); position-space renormalisation-group methods (Berker and Wortis 1976, Burkhardt 1976, Kaufman *et al* 1981, Yeomans and Fisher 1981) and series expansion (Saul *et al* 1974).

Mainly real-space renormalisation-group methods were employed for general q : a usual Niemeijer-van Leeuwen type type information (modifying the majority rule such that disorder cells be mapped onto a vacant cell site) on the triangular lattice (Nienhuis *et al* 1979); the Kadanoff variational approach in two (Nienhuis *et al* 1980a, Burkhardt 1980) and some other dimensions (Nienhuis *et al* 1981) and the Migdal bond-shifting method on d -dimensional hypercubic lattices (Berker *et al* 1980, Andelman and Berker 1981, Nienhuis *et al* 1981). The three-state Potts lattice-gas was used by Berker *et al* (1978) to obtain a picture of the multicritical phase diagram of monolayers, like krypton adsorbed on graphite, by using the Migdal renormalisation group on the triangular lattice.

It is well known from the work of Kasteleyn and Fortuin (1969) that the pure Potts model can be extended to continuous values of q , thus providing a formulation

of the bond percolation problem in the limit $q \rightarrow 1$. Following this procedure in the case of the diluted Potts model, the same limit produces the Ising-correlated site-bond percolation problem (Coniglio and Klein 1980, Wu 1981) first introduced to describe solvent effects on polymer gelation (Coniglio *et al* 1979, 1982). The behaviour of clusters and droplets near the critical point in a ferromagnetic Ising system can also be studied by means of this percolation model (Coniglio and Klein 1980).

The dilute q -state Potts model as given by (1) is equivalent, for vanishing magnetic field ($h = 0$), to the pure asymmetric $(q + 1)$ -state model defined as

$$\mathcal{H}' = -J' \sum_{(ij)} [(\delta_{s'_i, s'_j} - 1) + \alpha' (\delta_{s'_i, s'_j} \delta_{s'_i, 0} - 1)] - h' \sum_i (\delta_{s'_i, 0} - 1), \quad (4)$$

with $s'_i = 0, 1, \dots, q$ (Coniglio *et al* 1981). The correspondence between the parameters:

$$J = J', \quad \alpha = \alpha' + 2 \quad \text{and} \quad \mu = h' + c(\alpha' + 1)J', \quad (5)$$

where c is the coordination number of the lattice. Mainly the $q = 2$ case was studied extensively (which means the three-state model) by series expansion (Straley and Fisher 1973, Kim and Joseph 1975), Landau theory (Golner 1973, Straley and Fisher 1973, Rudnick 1975, Blankshtein and Aharony 1980) and momentum-space renormalisation-group (Golner 1973, Rudnick 1975, Blankshtein and Aharony 1980), while a large- q expansion was used by Goldschmidt (1981) to derive the phase boundary of the pure Potts model in a positive magnetic field ($h' > 0$). All these works, with the exception of the paper by Blankshtein and Aharony (1980), considered the symmetric model ($\alpha' = 0$).

The phase diagram of the diluted Potts model in zero magnetic field will be discussed in the present paper for general q and d , and also new results concerning the phase boundary will be given in some special cases. We are interested especially in multicritical behaviour and the possible existence of a tetracritical point in our system will be emphasised.

A concise version of this work focusing on the percolation problem can be found in Temesvári and Herényi (1983).

The outline of the paper is as follows. In § 2 exact results for the phase boundary are summarised and a new one in a limiting case of the interaction parameters is derived. The BEG model subjected to a constraint is mapped, on the honeycomb lattice, onto the pure Ising model, thus providing an exact intersection of the critical surface (§ 2.2). The phase boundary and the locations of multicritical points are determined on a Cayley tree in § 3. A discussion of the phase diagram and critical behaviour for general q and d is given in § 4. In § 5 the percolation problem ($q = 1$) is investigated in more detail. We argue that a tetracritical point might exist in the 3D correlated site-bond model, and scaling laws are used to derive the probably exact exponent of the mean cluster size when approaching the Ising critical point along the temperature axis in the 2D correlated site case.

2. Exact results for the phase boundary

2.1. General q and d

For completeness, we first review the known results. To establish the equivalence between the Potts lattice-gas and the models in equations (2) and (4), a correspondence

between states must be given as follows:

$$t = 0 \leftrightarrow \tilde{S} = 0 \leftrightarrow s' = 0$$

$$t = 1 \text{ and } s = 1 \leftrightarrow \tilde{S} = +1 \leftrightarrow s' = 1$$

$$t = 1 \text{ and } s = 2, \dots, q \leftrightarrow \tilde{S} = -1 \text{ for } q = 2 \leftrightarrow s' = 2, \dots, q.$$

Dividing the single-site terms among the incident bonds, we can rewrite the Hamiltonians (1), (2) and (4) in such a form that summations are only over nearest-neighbour interactions. Making equal the energies of all the possible bond configurations of figure 1 (only the $h = \tilde{H} = 0$ case is considered here) it follows that

$$\begin{aligned} \mathcal{H}_a &= 0, & \mathcal{H}_b &= \mu/c = \tilde{\Delta}/c = (\alpha' + 1)J' + h'/c, \\ \mathcal{H}_c &= -\alpha J + 2\mu/c = -\tilde{J} - \tilde{K} + 2\tilde{\Delta}/c = \alpha' J' + 2h'/c, & (6) \\ \mathcal{H}_d &= -(\alpha - 1)J + 2\mu/c = \tilde{J} - \tilde{K} + 2\tilde{\Delta}/c = (\alpha' + 1)J' + 2h'/c. \end{aligned}$$

Equations (3) and (5) are direct consequences of equation (6).

The ground-state properties, and thus the phase transition at zero temperature, can be easily deduced from (6). For $\mu < \frac{1}{2}c\alpha J$ ($\mu > \frac{1}{2}c\alpha J$) all the spins are in the same state (there are only vacancies in the system) when $T = 0$, thus a transition from the 'solid' to the 'gas' phase takes place at $\mu = \frac{1}{2}c\alpha J$. For $\mu = -\infty$ the density of vacancies vanishes and the pure q -state Potts Hamiltonian, with coupling constant J and magnetic field h , is obtained for all temperatures.

In an early paper, Griffiths (1967) pointed out that for $\tilde{J} = 0$ the BEG model can be mapped onto an Ising model in an external field. This can be easily generalised to $q \neq 2$. Let $J = 0$ but αJ finite in (1). After summing out the spin degrees of freedom, the partition function can be written as

$$Z = \sum_{\{t\}} \exp\left(\frac{\alpha J}{kT} \sum_{\langle ij \rangle} t_i t_j + \sum_i (\ln q - \mu/kT) t_i\right).$$

Introducing the Ising spins

$$\sigma_i = 2t_i - 1 \tag{7}$$

the following relations result

$$J_1 = \frac{1}{4}\alpha J \quad \text{and} \quad H_1 = \frac{1}{4}c\alpha J + \frac{1}{2}(kT \ln q - \mu),$$

with the Ising coupling J_1 and field H_1 . A first-order transition line for $H_1 = 0$ ending at the Ising critical point (which we will call the Griffiths point) must, therefore, be part of the whole phase diagram.

A new exact result can be derived for the limiting case $\alpha \rightarrow \infty$ while $H \equiv \frac{1}{2}c\alpha J - \mu$ remains finite. In this case, it follows from (6) that $\mathcal{H}_b \rightarrow \infty$, which means that configurations with adjacent vacancies and spins are excluded (see figure 1). The partition

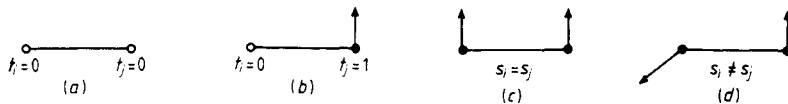


Figure 1. The four bond configurations with different interaction energies in the q -state Potts lattice-gas.

function can be separated into two parts:

$$Z = 1 + \exp\left(\frac{H}{kT}N\right) \sum_{\{s\}} \exp\left(\frac{J}{kT} \sum_{\langle ij \rangle} (\delta_{s_i, s_j} - 1) + \frac{h}{kT} \sum_i (\delta_{s_i, 1} - 1)\right),$$

where the first term comes from the 'gas' configuration with all $t_i = 0$ (N is the number of lattice sites). In the second term the partition function of the pure q -state Potts model has appeared; this can be expressed by means of the free energy per site f_{pure} in the usual way. Thus

$$Z = 1 + \left[\exp\left\{ \frac{1}{kT} \left[H - f_{\text{pure}}\left(\frac{J}{kT}, \frac{h}{kT}\right) \right] \right\} \right]^N.$$

In the thermodynamic limit ($N \rightarrow \infty$) we have two possibilities: for $H < f_{\text{pure}}$, $Z = 1$ and we are in the 'gas' phase, while for $H > f_{\text{pure}}$ there are no vacancies in the system. Figure 2 shows the phase diagram for $h = 0^+$ containing three phases. The first-order line $H = f_{\text{pure}}(J/kT, h = 0^+)$ separates the 'gas' phase from the two others, while, of course, there is a transition in the pure model whose order depends on q . For $q \leq q_c(d)$ the transition from the 'solid' to the 'liquid' phase is second order and the point E in figure 2 is a critical endpoint. The appearance of the latent heat for $q > q_c(d)$ means a break in the free energy function at the transition point, thus causing the three first-order transition lines to meet with three different slopes at E which now becomes a point of $(q + 2)$ -phase coexistence.

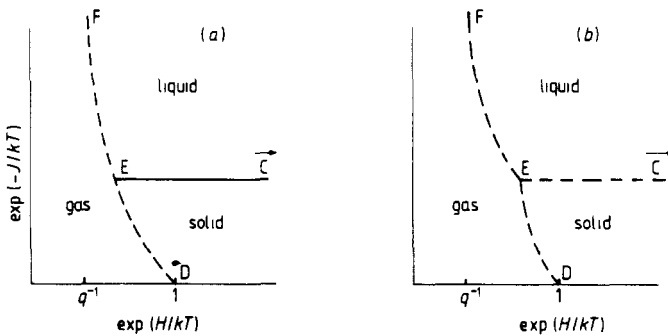


Figure 2. Schematic phase diagram of the diluted q -state Potts model in the limit $\alpha \rightarrow \infty$ and $H = \frac{1}{2}\alpha J - \mu$ is finite ($h = 0^+$). (a) $q \leq q_c(d)$. E is a critical endpoint. (b) $q > q_c(d)$. E is now a transition point with $(q + 2)$ -phase coexistence. Note the different slopes at E in this case. First- (second-) order transitions are drawn by broken (full) lines.

All the results of this subsection are summarised in table 1, where the new variables X , Y and Z are used instead of μ , α and J/kT :

$$\begin{aligned} X &\equiv \exp(-H/kT) = \exp[-(\frac{1}{2}\alpha J - \mu)/kT], \\ Y &\equiv \exp(-\alpha J/2kT) \quad \text{and} \quad Z \equiv \exp(-J/kT). \end{aligned} \tag{8}$$

Subsequently, it will be useful to express the equations for the phase boundary in terms of these parameters.

Table 1. Exactly known transition lines and points of the diluted q -state Potts model for general d and q . The definition of the variables X , Y and Z in terms of $H/kT = (\frac{1}{2}caJ - \mu)/kT$, α and J/kT can be found in equation (8). $T_c(q)$ and T_c are the critical temperatures of the pure q -state Potts and Ising models, respectively. Obviously $2J_1/kT_c = J/kT_c(q = 2)$. X_c is known exactly for some lattices in the case of $q = 1$, since it is connected with the random site percolational threshold.

Name	Notation	Definition	Nature of the transition
Pure q -state Potts line	BC	$X = 0,$ $Z = \exp(-J/kT_c(q))$	$q \leq q_c(d)$: second order $q > q_c(d)$: first order
	DF	$Y = 0,$ $X = \exp[-f_{\text{pure}}(-\ln Z, 0^+)/kT]$	first order
	CE	$Y = 0,$ $Z = \exp(-J/kT_c(q))$	$q \leq q_c(d)$: second order $q > q_c(d)$: first order
Griffiths-line Zero-field transition line in the symmetric $(q + 1)$ -state Potts model	FG	$X = q, Z = 1$	first order
	DY	$X = 1, Z = Y$ $(\alpha' = \alpha - 2 = 0, h' = 0)$	first order
Zero-temperature transition points	D	$X = 1, Y = 0, Z = 0$ $(\alpha > 0)$	first order
	A	$X = X_c, Y = 1, Z = 0$ $(\alpha = 0)$	$q \leq q_c(d)$: second order $q > q_c(d)$: first order
	C	$X = 0, Y = 0,$ $Z = \exp(-J/kT_c(q))$	$q \leq q_c(d)$: second order $q > q_c(d)$: first order
	E	$X = \exp\left(\frac{-f_{\text{pure}}(J/kT_c(q), 0^+)}{kT_c(q)}\right)$ $Y = 0,$ $Z = \exp(-J/kT_c(q))$	$q \leq q_c(d)$: critical endpoint $q > q_c(d)$: $(q + 2)$ -phase coexistence
	F	$X = q, Y = 0, Z = 1$	first order
Griffiths-point	G	$X = q,$ $Y = \exp(-2J_1/kT_c), Z = 1$	second order
	Y	$X = 1,$ $Y = Z = \exp[-J/kT_c(q + 1)]$ $(\alpha' = \alpha - 2 = 0, h' = 0)$	$q \leq q_c(d) - 1$: second order $q > q_c(d) - 1$: first order

2.2. Exact mapping of a special case of the honeycomb Blume–Emery–Griffiths model onto the pure Ising model

Transformations, such as e.g. the decoration, dedecoration and star–triangle, have long been useful in establishing relationships between different lattice models. Their common property is that the Boltzmann weights of corresponding configurations are left unchanged (or more precisely, they are multiplied by a constant) under this transformation by suitably relating the parameters of the two models. For lattices with coordination number three, a correspondence between the BEG and pure Ising models can be found by similar steps of transformations (see figure 3).

Firstly the interactions of the BEG (or diluted two-state) model are decorated by the usual $\sigma = \pm 1$ Ising spins. From the relations between the corresponding Boltzmann weights of all the possible four bond configurations, we obtain

$$\cosh 2\tilde{J}'/kT = \exp(2\tilde{J}/kT), \quad \exp(\tilde{\Delta}'/kT) = \exp\{[\tilde{\Delta} + \frac{3}{2}(\tilde{J} - \tilde{K})]/kT\} \tag{9}$$

and

$$\exp(-\tilde{K}/kT) = \cosh(\tilde{J}/kT). \tag{10}$$

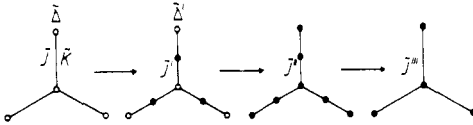


Figure 3. The series of transformations for finding the correspondence between a Blume-Emery-Griffiths model with the constraint $\exp(-\tilde{K}/kT) = \cosh(\tilde{J}/kT)$ and the pure Ising model on lattices with coordination number three. Open circles are for $\tilde{S} = 0, \pm 1$, while full circles are for $\sigma = \pm 1$ Ising spins.

The constraint for the BEG model in (10) is needed since the original equations are overdetermined. Extending these considerations to the general q case, in order to establish a condition of being able to decorate a bond of the diluted model by a pure Potts spin, we could obtain an equation which is also the constraint for the diluted Potts model to have a pure dual with multispin interactions (Wu 1981).

The \tilde{S} spins at the vertices are replaced by σ spins in the second step. We notice this can be made only for the two-state case since otherwise the number of different configurations of the Potts spins surrounding a vertex would be three instead of two. It is straightforward to obtain:

$$2 \cosh \frac{2\tilde{J}''}{kT} = 1 + \frac{1 + 2 \exp(-\tilde{\Delta}'/kT) \cosh(3\tilde{J}'/kT)}{1 + 2 \exp(-\tilde{\Delta}'/kT) \cosh(\tilde{J}'/kT)}. \quad (11)$$

Finishing the procedure, a simple dedecoration provides the pure Ising model:

$$\exp(2\tilde{J}'''/kT) = \cosh(2\tilde{J}''/kT). \quad (12)$$

From (9)-(12), the mapping between the constrained BEG and pure Ising models follows:

$$\exp\left(\frac{2\tilde{J}'''}{kT}\right) = 1 + \frac{4 \sinh(\tilde{J}/kT)}{\exp(\tilde{\Delta}/kT) \cosh(\tilde{J}/kT) + 2 \exp(-\tilde{J}/kT)}, \quad (13)$$

which is valid when (10) is fulfilled.

An intersection of the phase boundary of the BEG model is obtained by taking the exactly known critical condition for the Ising model on the left-hand side of equation (13). Returning to the variables defined in (8) and using (3), the constraint in (10) becomes

$$Y^2 = \frac{1}{2}(1 + Z) \quad (14)$$

and the critical condition from (13) for the honeycomb lattice (for a Cayley tree with branching ratio two) is

$$Z/(1 - Z) + X(1 + Z)/4Y^3(1 - Z) + 1/(1 + \sqrt{3}) \quad (= \frac{1}{2}) \quad (15)$$

Since under transformation (13) only an irrelevant constant is added to the free energy, the constrained BEG model has a continuous transition along the critical surface given by (14) and (15) and belongs to the universality class of the pure Ising model.

3. Multicritical behaviour on the Cayley tree

To obtain a picture of the topology of the phase diagram, we locate first-order, critical and multicritical points in the case of the Cayley tree (or Bethe lattice). We must,

however, proceed with some caution; a Cayley tree has a finite surface to volume ratio in the thermodynamic limit (therefore, it can be considered in some sense as an infinite-dimensional lattice), thus boundary effects may be essential in determining thermodynamic properties. In contrast with the case of regular lattices, here it is important how the single-site variables in the Hamiltonian are divided between the incident bonds. Since our goal is to imitate the phase diagram on regular lattices, all the exact results of § 2.1 must be preserved. The correct zero-temperature transition at $H = \frac{1}{2}\alpha J - \mu = 0$ can be obtained by the following regrouping of Hamiltonian (1)

$$\mathcal{H} = -J \sum_{(ij)} [(\delta_{s_i, s_j} - 1)t_i t_j + \alpha t_i t_j - \frac{1}{2}\alpha(t_i + t_j)] - \sum_i [H + h(\delta_{s_i, 1} - 1)]t_i. \quad (16)$$

It is easy to check that the line DF of table 1 is also reproduced in this way (which is not the case when the Hamiltonian is left in the form of equation (1)).

Another difficulty arises when we try to define the order parameters. For regular lattices, the following definitions seem to be convenient:

$$m_1 \equiv \frac{q}{q-1} N^{-1} \sum_i (\langle t_i \delta_{s_i, 1} \rangle - q^{-1} \langle t_i \rangle) = \frac{q}{q-1} (\langle t_0 \delta_{s_0, 1} \rangle - q^{-1} \langle t_0 \rangle)$$

and (17)

$$m_2 \equiv \frac{q+1}{q} N^{-1} \sum_i [\langle (1-t_i) - (q+1)^{-1} \rangle] = \frac{q+1}{q} [\langle (1-t_0) - (q+1)^{-1} \rangle],$$

where $\langle \dots \rangle$ denotes the thermal average. Here $m_1(m_2)$ is the q -state Potts (the lattice-gas) order parameter and the homogeneity of the lattices was utilised in deriving the second equations (the index "0" refers to the site at the origin). This homogeneity, however, is absent in the case of the Cayley tree. For the pure Ising and Potts models, the spontaneous magnetisation was found to be zero for all temperatures, while the averages at the origin showed the usual behaviour of an order parameter vanishing at the transition point with mean-field exponents (Eggarter 1974, Wang and Wu 1976). Therefore, we adopt, as the definition of the order parameters, the second parts of equation (17).

The method of calculating thermodynamic functions on Cayley trees is well known (see e.g. Eggarter 1974, Wang and Wu 1976): the summation over surface variables can be performed successively, renormalising the single-site parameters at the boundary in each step. The procedure is shown in figure 4 and the recursive equations are easily derived. Making equal the Boltzmann weights for the three different single-site states $t=0$, $s=1$ and $s>1$ we obtain

$$\begin{aligned} A_{n+1} &= A_n^{c-1} \{1 + \exp[(H_n - \frac{1}{2}\alpha J)/kT][1 + (q-1)\exp(-h_n/kT)]\}^{c-1} \\ A_{n+1} \exp(H_{n+1}/kT) &= A_n^{c-1} [1 + \exp[(H_n + \frac{1}{2}\alpha J)/kT] \\ &\quad \times \{1 + (q-1)\exp[-(J+h_n)/kT]\}]^{c-1} \exp\{[H - \frac{1}{2}(c-1)\alpha J]/kT\} \\ A_{n+1} \exp[(H_{n+1} - h_{n+1})/kT] &= A_n^{c-1} [1 + \exp[(H_n + \frac{1}{2}\alpha J)/kT] \\ &\quad \times \{\exp(-J/kT) + \exp(-h_n/kT) \\ &\quad + (q-2)\exp[-(J+h_n)/kT]\}]^{c-1} \exp\{[H - h - \frac{1}{2}(c-1)\alpha J]/kT\}, \end{aligned}$$

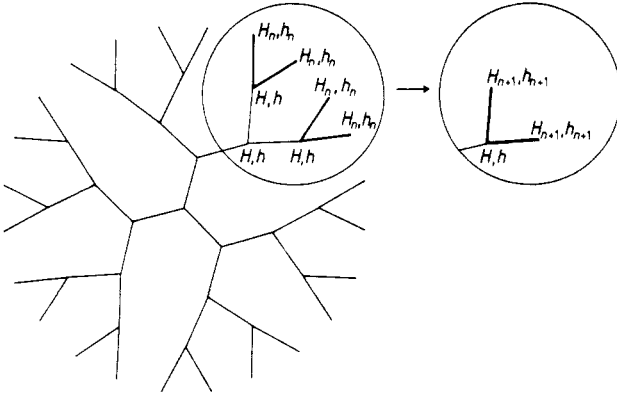


Figure 4. Cayley tree (or Bethe lattice) with branching ratio two ($c = 3$) showing the method how the recursion relations of equation (18) are obtained: after summing over the variables in the n th generation (surface sites), the single-site parameters (H and h) of the $(n + 1)$ th generation will be renormalised.

where the multiplicative factors, A_n and A_{n+1} , are important only for the calculation of the partition function and $c - 1$ is the branching ratio of the Cayley tree. The recursion formula for H_n and h_n , using the variables of equation (8), is then given by

$$X_{n+1} = X \left(\frac{X_n + Y[1 + (q - 1) \exp(-h_n/kT)]}{X_n Y + 1 + (q - 1) Z \exp(-h_n/kT)} \right)^{c-1}, \tag{18}$$

$$\exp(-h_{n+1}/kT) = \exp(-h/kT) \left(\frac{X_n Y + Z + [1 + (q - 2)Z] \exp(-h_n/kT)}{X_n Y + 1 + (q - 1) Z \exp(-h_n/kT)} \right)^{c-1}.$$

In the thermodynamic limit, eliminating all the degrees of freedom but those at the origin and its surrounding sites, the field variables go to a fixed point X^* , h^* . As a last step, equation (18) is used with c , instead of $c - 1$, and $X_n = X^*$, $h_n = h^*$ to obtain a single site with $X_{\text{eff}} = \exp(-H_{\text{eff}}/kT)$ and h_{eff} . The partition function and the order parameters can be expressed by the effective fields:

$$Z = A_{\text{eff}} \{ 1 + \exp(H_{\text{eff}}/kT) [1 + (q - 1) \exp(-h_{\text{eff}}/kT)] \},$$

$$m_1 = \exp(H_{\text{eff}}/kT) \frac{1 - \exp(-h_{\text{eff}}/kT)}{1 + \exp(H_{\text{eff}}/kT) [1 + (q - 1) \exp(-h_{\text{eff}}/kT)]} \tag{19}$$

and

$$m_2 = \frac{1 - q^{-1} \exp(H_{\text{eff}}/kT) [1 + (q - 1) \exp(-h_{\text{eff}}/kT)]}{1 + \exp(H_{\text{eff}}/kT) [1 + (q - 1) \exp(-h_{\text{eff}}/kT)]}.$$

From now on only the $c = 3$ case will be considered. For vanishing magnetic field there is a fixed point X_0^* , $h^* = 0$, where X_0^* can be calculated from (18):

$$X_0^* = X \left(\frac{X_0^* + qY}{X_0^* Y + 1 + (q - 1)Z} \right)^2. \tag{20}$$

From equation (20) we can deduce that a first-order lattice-gas transition takes place in two cases: (i) when the initial value X gets from the region of attraction of one fixed point to that of another and (ii) when an attractive fixed point becomes marginal

and finally disappears causing an abrupt change in H_{eff} . The location of these two types of lattice-gas transition in the 3D parameter space X , Y and Z can be easily determined by straightforward algebra from equation (20); the results are given in the first two rows of table 2.

Table 2. Transition surfaces, lines and points for the q -state Potts lattice-gas on a Cayley tree with branching ratio two ($1 \leq q < 2$). The notation $u \equiv q^{-1}[1 + (q - 1)Z]$ is used. There is first-order q -state Potts transition also on a part of the lattice-gas surface bounded by the lines EY, YJ, JK, KD and DE.

Name and/or notation	Boundary lines or points	Defining equation
Lattice-gas transition surface (with fixed point changing)	GF, FD, DH and HG	$X = q(u - Y)/(1 - Y) \equiv X_{LG}$
Lattice-gas transition surface (with a marginal fixed point)	GH, HI and IG	$X = \frac{qu(u + 3Y^2 + v)^2}{8Y(u - 3Y^2 + v)} \equiv X'_{LG}$ with $v \equiv (u^2 - 10uY^2 + 9Y^4)^{1/2}$
q -state Potts transition surface	BC, CE, EY, YJ, JK, KA and AB	$X = \frac{4qY(1 - u)^2[2 - (q + 1)u]}{(q - 1)[2 - (q + 1)u + (q - 1)Y^2]^2} \equiv X_{\text{Potts}}$
Lattice-gas critical line	I and G	$u = 9Y^2$ and $X = 27qY^3$
Tricritical line	Y and J	$Y^2 = Z[2 - (q + 1)u]/[3 - (q + 2)u]$ and $X = X_{\text{Potts}}$
Line separating the two types of lattice-gas surfaces	H and G	$u = Y(2 - 3Y)/(1 - 2Y)$
Line of type-I critical endpoints	J and K	$X = X_{\text{Potts}} = X'_{LG}$ and $X = X_{\text{Potts}} = X_{LG}$
Line of type-II critical endpoints	E and Y	$X = X_{\text{Potts}} = X_{LG}$
Pure $(q + 1)$ -state Potts transition point (Y)		$X = 1$ ($\alpha = 2$)
Tetracritical point (J)		$Y^2 = [3(2q + 1)]^{-1}$ ($\alpha = 1 + \ln 3/\ln(2q + 1)$)
E		$Y = 0$
K		$Z = 0$
I		$Z = 0$
G		$Z = 1$

The lattice-gas ordering is not the only phase transition in the model. The zero-field fixed point we have just obtained may be unstable against a small perturbation of the magnetic field: the q -state Potts ordered phase is characterised by a finite-field fixed point giving rise to a non-vanishing m_1 in equation (19). The stability condition can be derived from (18):

$$\partial h_{n+1}/\partial h_n = 1 + C_1, \quad h = 0$$

with

$$C_1 = 2(1 - Z)/[X_0^* Y + 1 + (q - 1)Z] - 1. \tag{21}$$

Here $C_1 > 0$ ($C_1 < 0$) means the ordered (disordered) phase and there is a q -state Potts transition at $C_1 = 0$ (see table 2). C_1 changes sign also at a section of the lattice-gas surface bounded by the lines EY, YJ, JK, KD and DE because of the discontinuity in X_0^* (see table 2 for notation). This abrupt change causes simultaneous q -state Potts and lattice-gas transitions which are, of course, first order.

Near the Potts transition ($C_1 \approx 0$) there is always a fixed point with $h^* \approx 0$ in addition to that with $h^* = 0$. It can be determined from the following series derived directly from equation (18):

$$C_1(h^*/kT) + C_2(h^*/kT)^2 + C_3(h^*/kT)^3 + \dots = 0, \tag{22}$$

where the coefficients are functions of X, Y, Z and C_1 is explicitly given in (21). Thus the finite-field fixed point takes the form

$$h^*/kT = -C_1/C_2,$$

where C_2 must be taken at the critical surface. After a lengthy calculation, C_2 proved to be constant on the whole Potts transition surface leading to

$$h^*/kT = -4qC_1/(q-2). \tag{23}$$

As it turns out, the finite-field fixed point with $h^* \approx 0$ is positive and stable in the ordered phase only for $q < 2$ (stability can be easily checked by means of equation (18)), while h^* (and thus also h_{eff}) is finite even at the Potts transition for $q > 2$ giving rise to a discontinuity of m_1 on the whole phase boundary in this case. Hence we conclude that $q_c = 2$ on the Cayley tree. Details of the phase diagram will be presented for the three different cases separately.

3.1. $1 < q < 2$

For given J, α and μ the order parameter critical exponent β can be defined, using (19) and (23), as follows:

$$m_1 \sim h_{\text{eff}} \sim h^* \sim C_1 \sim |T - T_c|^\beta,$$

where the absolute value is needed since for some α 's, as will be shown, ordering may occur above T_c . It follows from equation (21) that X_0^* approaches its critical value (for fixed J, α and μ) with the same exponent β . Therefore, we can determine β by investigating the cubic equation (20).

The results for the phase diagram are summarised in table 2 and its topology is shown in figure 7(a). Three different values were obtained for the critical index β : (i) $\beta = 1$ on the q -state Potts surface and along the lines of critical endpoints; (ii) $\beta = \frac{1}{2}$ along the tricritical line; (iii) $\beta = \frac{1}{3}$ in the tetracritical point. The tricritical line, as contrasted with the $q = 2$ case, coincides with the intersection of the q -state Potts and lattice-gas transition surfaces. This can be seen in figure 5(c), where the phase diagram shows a tricritical point which is also the origin of the lattice-gas transition line, very similarly to critical endpoints on JK and EY (figure 5(a) and (e)). There are, however, two essential differences: first $\beta = 1$ along JK and EY, secondly the three lines intersect with the same slope at a tricritical point, which is not true for critical endpoints. A critical endpoint on JK (EY) is called type-I (type-II) in this paper. A phase diagram containing a type-I critical endpoint (figure 5(a)) has the property that the lattice-gas critical point is in the ordered phase where $m_1 > 0$ (see also Ziman *et al* (1982), where this type of critical endpoints was investigated in the Ising case). The process of how

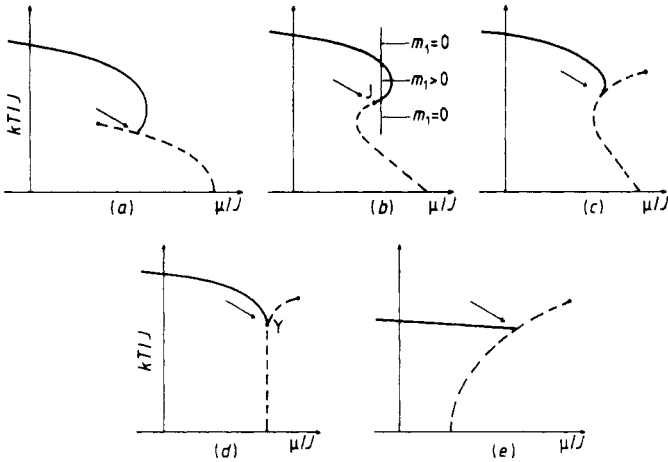


Figure 5. Phase diagram of the diluted Potts model on a Cayley tree with branching ratio two for different values of α ($1 < q < 2$). Broken (full) lines are for first- (second-) order transitions. The arrows denote: (a) a type-I critical endpoint ($\alpha < \tilde{\alpha}$); (b) the tetracritical point ($\alpha = \tilde{\alpha}$); (c) a tricritical point ($\tilde{\alpha} < \alpha < 2$); (d) the pure $(q + 1)$ -state Potts transition point ($\alpha = 2$); (e) a type-II critical endpoint ($\alpha > 2$). For a range of the parameter α an intermediate temperature region with non-zero-order parameter ($m_1 > 0$) appears. This is shown by the vertical line crossing the ordered phase in (b).

different types of multicritical points follow each other when changing α is shown in figure 5: a type-I critical endpoint becomes a tricritical point through the tetracritical point at

$$\tilde{\alpha} = 1 + \ln 3 / \ln(2q + 1),$$

while the type-II critical endpoints take their origin at the pure $(q + 1)$ -state Potts transition point for $\alpha = 2$. The tetracritical point and the pure $(q + 1)$ -state Potts transition point are on the lattice-gas critical line (IG) and on the line separating the two different regions of the lattice-gas transition surface (HG), respectively (see figure 7(a)). We call attention to the strange phenomenon which can be observed for an interval of the parameter α (see e.g. figure 5(b)): there is an ordered q -state Potts-phase in an intermediate temperature range with two critical transitions!

We are especially interested in the case $\alpha = 2$ (see figure 5(d)) when, according to (4) and (5), the pure $(q + 1)$ -state Potts model is obtained. In the region we are investigating $(q + 1) > q_c = 2$ and the transition must be first order, which is indeed the case since m_2 has a discontinuity at the zero-field transition point. An interesting thing happens, however, if we consider the susceptibility χ_2 defined, together with χ_1 , by

$$\chi_1 \equiv \partial m_1 / \partial h \quad \text{and} \quad \chi_2 \equiv \partial m_2 / \partial (\mu + h).$$

Since the q -state Potts critical surface persists up to the $(q + 1)$ -state transition point, χ_1 diverges even at Y . But all the $(q + 1)$ states are equivalent for $\alpha = 2$, $H = h = 0$ and thus χ_2 must also diverge at Y . This phenomenon, a discontinuity in the order parameter and divergence of the susceptibility, has been found by series expansion in lower dimensionalities (Kim and Joseph 1975). Here it is the consequence that the tricritical line terminates in Y instead of a type-II critical endpoint. The intersection of the lattice-gas critical line (IG) and the $\alpha = 2$ subspace gives the critical point for $h' > 0$ ($H < 0$) which is thus Ising-type.

3.2. $q > 2$

All the manifolds of the phase diagram listed in table 2 are present but with a different character: there are first-order transitions everywhere except along IG. Along YJ, for example, $(q + 2)$ phases coexist and it is not any more a line of tricritical points.

3.3. $q = 2$

Since $C_2 \equiv 0$ on the whole two-state Potts transition surface the third-order term must be taken into account in the expansion of equation (22). Thus

$$h^*/kT = (-C_1/C_3)^{1/2}$$

and it is real in the ordered phase ($C_1 > 0$) if $C_3 < 0$. In this case the transition is continuous and $\beta = \frac{1}{2}$, which is the well known Ising mean-field exponent. C_3 , in contrast with C_2 , is not constant on the phase boundary and $C_3 = 0$ defines the tricritical line, which can be obtained from equation (18):

$$Y^2 = (1 + Z)(3Z - 1)/2(5Z - 3).$$

It lies, of course, on the two-state Potts transition surface (which can be taken from table 2 with $q = 2$) but it is not its boundary. This tricritical line terminates on the line of type-II critical endpoints (a property found previously in mean-field calculations for the BEG model (Blume *et al* 1971, Mukamel and Blume 1974, Berker and Wortis 1976, Furman *et al* 1977, Blankschtein and Aharony 1980)) for

$$\alpha = 2.358.$$

Phase diagrams for different α 's are shown in figure 6: tricritical points are now separated from quadruple points and the three-state Potts transition point itself (Y for $\alpha = 2$, see figure 6(d)) is a quadruple point (Straley and Fisher 1973). All the results for $q = \alpha = 2$ agree with those of Baumgärtel and Müller-Hartmann (1982)

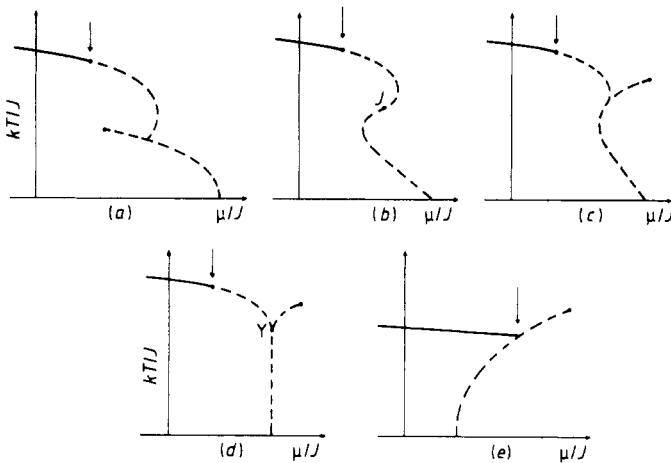


Figure 6. Phase diagram of the two-state diluted Potts model (i.e. Blume–Emery–Griffiths model) on a Cayley tree with branching ratio two for different values of α : (a) $\alpha < \tilde{\alpha}$; (b) $\alpha = \tilde{\alpha}$; (c) $\tilde{\alpha} < \alpha < 2$; (d) $\alpha = 2$; (e) $\alpha > 2$. Broken (full) lines are for first- (second-) order transitions. The arrows denote tricritical points in all cases except (e), where a type-II critical endpoint is shown. The sort of phase diagrams shown in (a) has not been obtained, to our knowledge, by mean-field methods.

who studied the symmetric Potts model on a Cayley tree. Also the line derived in § 2.2, equations (14) and (15), for the Cayley tree with coordination number three is reproduced and found to be entirely on the critical surface.

We must take note of the discontinuity of the phase diagram at $q = q_c = 2$, a property which is missing in lower dimensions. We can, however, refer to the similar discontinuity in the mean-field critical exponents α and β : $\alpha = -1$, $\beta = 1$, for $q < 2$ and $\alpha = 0$, $\beta = \frac{1}{2}$ for $q = 2$. Since the changeover in the nature of the phase transition occurs at $q_c = 2$ for all dimensions larger than four (Wu 1982), we think the discontinuity property found on the Cayley tree is true for all $d > 4$.

4. Discussion

Some properties of the phase diagram in lower dimensions can be deduced from the exact results of § 2, the Cayley tree solution of § 3 and approximate calculations in the literature.

The appearance of a new type of lattice-gas transition (with a marginal fixed point) for $q > 1$ on the Cayley tree ensured the changeover in the nature of the pure $(q + 1)$ -state Potts transition at $q = q_c(\infty) - 1 = 1$. Perhaps this mechanism is also present on regular lattices. In this case the pure $(q + 1)$ -state Potts transition point lies on the line separating the two types of lattice-gas transition surface (terminates the lattice-gas critical line) for $q > q_c - 1$ ($q \leq q_c - 1$).

Nienhuis *et al* (1981) found, using the Kadanoff variational renormalisation-group method in investigating the diluted Potts model that for $d = 2.32$, the third thermal eigenvalue of the tricritical fixed point was relevant if q was less than some q_m ($1 < q_m < 2$). Thus the originally tricritical fixed point became a tetracritical one with three relevant thermal eigenvalues and Nienhuis *et al* (1981) argued that tricritical behaviour was governed by a Gaussian fixed point leading to classical tricritical exponents for $q < q_m$. We can naturally identify their $q_m(d)$ with the value where the type-I critical endpoints terminating at the tetracritical point appear and simultaneously tricritical behaviour becomes classical. On the Cayley tree ($d = \infty$) $q_m = 2$ and we conjecture this may be true for all $d > 3$, since in the BEG model the upper tricritical dimensionality is three. A type-I critical endpoint has been found in the special case of three-dimensional correlated site percolation ($q = 1$ and $Z = 0$): the ordered phase with an infinite cluster contains the Ising (or lattice-gas) critical point and the system begins to percolate on the coexistence curve below the Ising critical temperature (Müller-Krumbhaar 1974, Sykes and Gaunt 1976). Taking into account all the above considerations, $q_m(d)$ can be drawn schematically as in figure 8. With the analogy of $q_c(d)$ we expect that the phase diagram changes continuously along $q_m(d)$ for $d < 3$: the tetracritical point appears at $Z = 0$ and moves toward larger Z values as q is decreased from q_m . It would be interesting to examine in detail the 3D BEG model since, according to our prediction, it should have a tetracritical point at $Z = 0$.

The phase diagram for $q_m(d) < q \leq q_c(d) - 1$ seems to be well described by the renormalisation-group studies enumerated in the introduction. Thus the lattice-gas and q -state Potts surfaces have two intersections: the line of type-II critical endpoints (EY) and the tricritical line (YI). As usual, in the case of tricritical points, the two surfaces merge smoothly along YI.

We finish with some remarks concerning the phase diagram of the pure $(q + 1)$ -state Potts model of Hamiltonian (4) in the symmetric case $\alpha' = 0$. If the divergence of the

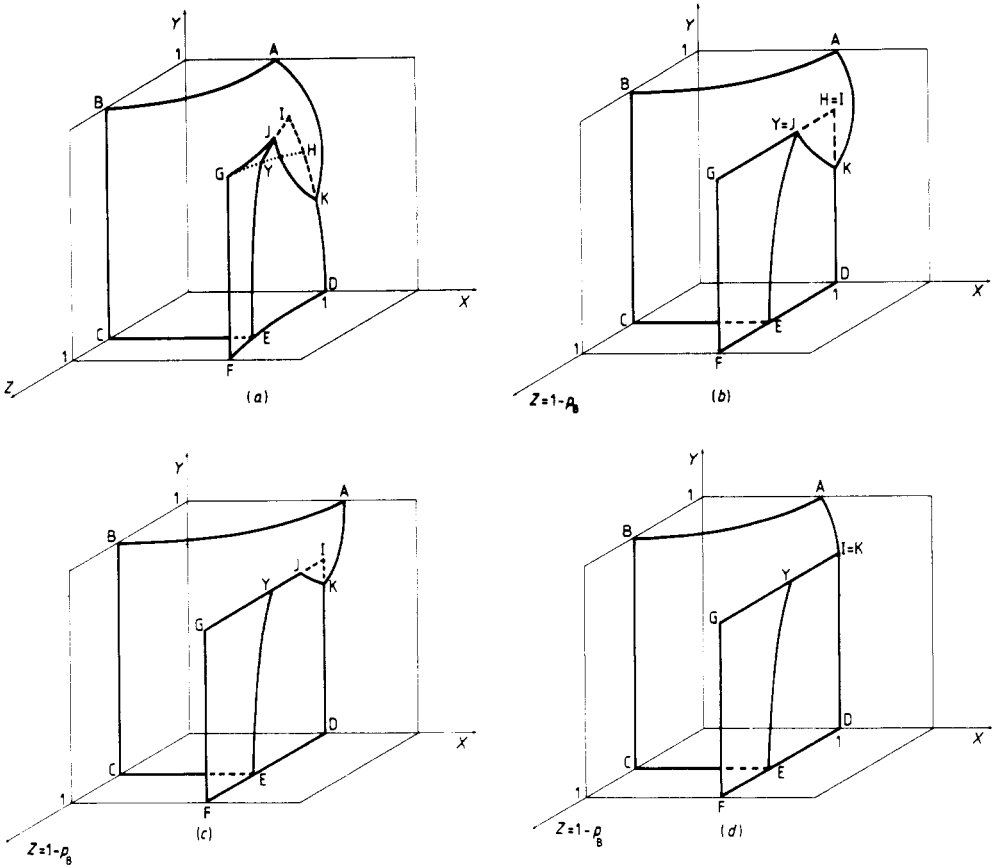


Figure 7. The topology of the phase diagram (see tables 1 and 2 for the notations used). (a) Exact result for the Cayley tree ($c = 3$) in the case $1 < q < 2$. The broken line (GH) separates the two types of lattice-gas transition; (b) Exact result for the Cayley tree ($c = 3$) in the case of percolation ($q = 1$). The tetracritical point (J) and the transition point where Ising droplets diverge (Y) coincide. The lattice-gas transition surface with the marginal fixed point disappears at $q = 1$ ($H = I$); (c) Conjectured phase diagram for three-dimensional percolation. The tricritical line YJ is expected to have classical exponents; (d) Two-dimensional case of percolation. The Ising critical point I is now also the place where the system begins to percolate ($I = K$). YI is the one-state Potts tricritical line.

susceptibility (Kim and Joseph 1975) and the specific heat (Binder 1981) at the zero-field transition point were true for $q > q_c(d) - 1$, in spite of the discontinuity in the order parameter and energy, it would suggest the phase diagram of figure 5(d) without a tricritical point (as compared with figure 6(d)) in two and three dimensions as well as on the Cayley tree. This would mean that the line of tricritical points should terminate at Y rather than on the line of type-II critical endpoints not only on the Cayley tree but also in lower dimensions. The critical point in positive field was found to be Ising type in the large- q limit (Goldschmidt 1981). Since in all renormalisation-group investigations (Berker and Wortis 1976, Berker *et al* 1978, 1980, Coniglio and Klein 1980, Andelman and Berker 1981, Kaufman *et al* 1981, Yeomans and Fisher 1981) the lattice-gas critical line was governed by the Griffiths point and it is exactly Ising type (see § 2.1); this property is probably true for all $q > q_c(d) - 1$.

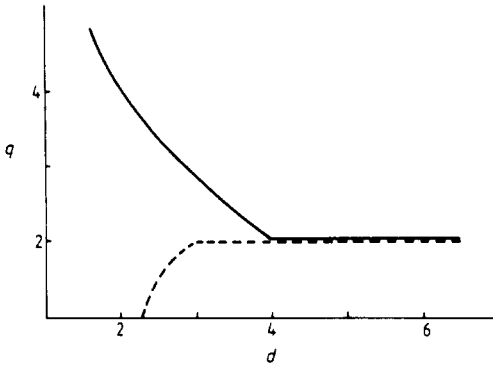


Figure 8. $q_c(d)$ and $q_m(d)$ are drawn schematically with full and broken lines, respectively. For $q \leq q_m(d)$ a tetracritical point can be found in the system and tricritical behaviour should be classical. At $q_c(d)$ the nature of the Potts transition changes from second to first order (taken from Wu (1982)).

5. Correlated site-bond percolation

The diluted Potts model describes Ising-correlated site-bond percolation in the limit $q \rightarrow 1$ (Coniglio and Klein 1980, Wu 1981). Now, the atoms do not occupy the lattice sites randomly, but different configurations are weighted by the Boltzmann factors $\exp(-\mathcal{H}_{LG}/kT)$ with the lattice-gas Hamiltonian

$$\mathcal{H}_{LG} = -\alpha J \sum_{(ij)} t_i t_j + \mu \sum_i t_i.$$

Eventually bonds are introduced between nearest-neighbour occupied sites randomly with the probability (Kasteleyn and Fortuin 1969, Coniglio and Klein 1980, Wu 1981)

$$p_B = 1 - \exp(-J/kT) = 1 - Z. \tag{24}$$

Because of its relevance to describe solvent effects on the sol-gel transition, this model was intensively investigated on the Cayley tree (Coniglio 1975, 1976, Coniglio *et al* 1979, 1982, di Liberto *et al* 1983). We analyse the phase diagram, using the results of § 3, as the limit $q = 1^+$ of the diluted Potts model (figure 7(a) and (b)). Conjecture and exact results will also be presented for the two- and three-dimensional cases (figure 7(c) and (d)).

The lattice-gas surface with the marginal fixed point vanishes just at $q = 1$ on the Cayley tree and phase separation occurs, independently of p_B , for

$$X = 1 \quad \text{and} \quad Y < \frac{1}{3},$$

where the Ising critical value of the parameter Y was used. This result is also true in lower dimensions but, of course, $\frac{1}{3}$ must be exchanged with the Ising critical value of the given regular lattice.

The $(q+1)$ -state Potts transition point and the tetracritical point, as can be seen in figure 7(a) and (b), join together at $q = 1$ forming a new multicritical point where critical ‘droplets’ diverge (Coniglio and Klein 1980) for

$$X = 1, \quad Y = \frac{1}{3} \quad \text{and} \quad p_B = \frac{2}{3}.$$

As a result, on the Cayley tree both type-I and type-II critical endpoints take their origin at this point, which lies in the $\alpha = 2$ subspace having attracted much interest in

recent years (Kertész *et al* 1982 and references therein) because it proved to be a good candidate for describing clusters (which are called droplets here) diverging at the Ising critical point T_c with Ising exponents (Coniglio and Klein 1980). Indeed, it can be verified using (20) with $q = 1$ and in the vicinity of the 'droplet' critical point that the percolational probability P which is proportional to m_1 (Coniglio and Klein 1980, Wu 1981) vanishes with the mean-field Ising exponent when approaching the 'droplet' critical point:

$$P \sim m_1 \sim (T_c - T)^{1/2}.$$

The type-I critical endpoint K can be found in the subspace of correlated site percolation ($p_B = 1$) and corresponds to the percolational temperature T_p on the coexistence curve below the Ising critical temperature T_c belonging to the point I (see figure 7(b)). We obtained

$$T_p/T_c = 0.9014,$$

which can be compared with the 3D value 0.96 (Müller-Krumbhaar 1974, Stauffer 1981, Heermann and Stauffer 1981). The random site-bond percolational surface can also be easily derived for the Cayley tree from table 2 taking $Y = 1$ and using the site probability (Coniglio and Klein 1980, Wu 1981)

$$p_s = (1 + X)^{-1}$$

and (24):

$$p_s p_B = \frac{1}{2} = 1/(c - 1).$$

In two dimensions $q_m(2) < 1 < q_c(2) - 1 = 3$ and the phase diagram looks like that described in § 4. As can be seen in figure 7(d), the Ising critical point I of correlated site percolation is also the place where an infinite network of neighbouring atoms appears (Coniglio *et al* 1977, Coniglio and Klein 1980) and it is actually a one-state Potts tricritical point. Using this fact, the exponent γ_p of the mean cluster size when approaching the Ising critical point along the temperature axis ($X = 1$) can be derived from the extended den Nijs' conjectures. From the usual scaling law $\gamma_p = (2 - \eta)\nu$ we can calculate γ_p using the probably exact values for the thermal and magnetic eigenvalues of the tricritical fixed point (den Nijs 1979, Nienhuis *et al* 1979, 1980b, Pearson 1980, Nienhuis 1982):

$$\nu = y_{T_2}^{-1} = 1 \quad \text{and} \quad 2 - \eta = 2y_h - d = \frac{91}{48}.$$

Thus

$$\gamma_p = \frac{91}{48} = 1.896 \quad (d = 2, p_B^Y < p_B \leq 1),$$

where p_B^Y is the bond probability at the droplet critical point. This can be compared with the series result $\gamma_p = 1.91 \pm 0.01$ (Sykes and Gaunt 1976) and renormalisation-group value $\gamma_p = 1.89$ (Coniglio and Klein 1980). γ_p differs, of course, from both the Ising and random percolational exponents of the susceptibility and mean cluster size. Although the scaling law used here has been stated by Coniglio and Klein (1980), they did not identify the Ising critical point with the $q = 1$ Potts tricritical point.

The 3D phase diagram is very similar to that of the Cayley tree with one essential difference (compare figures 7(c) and (b)): from the continuity argument of § 4 we expect that the tetracritical point and the two-state Potts transition point (which is now the droplet critical point) have not merged at $q = 1$ and $d = 3$. This would mean

that a separate tetracritical point might be found in the system at a bond probability p_B^J with $p_B^Y < p_B^J < 1$. We think that figure 4 in the paper of Heermann and Stauffer (1981) supports this idea: p_B for the two types of critical endpoints are shown as functions of the temperature and the two curves do not meet at the Ising critical temperature. However, in the discussions of the Monte Carlo results a phase diagram similar to that on the Cayley tree ($p_B^J = p_B^Y$) was always suggested (Stauffer 1981, Heermann and Stauffer 1981, Kertész *et al* 1982). Further Monte Carlo work would be useful in investigating this point.

According to the discussion of § 4 a line of classical tricritical points connects the tetracritical and droplet critical points. γ_p along this line can be calculated from the classical tricritical exponents:

$$y_{T2} = 1 \quad \text{and} \quad \eta = 0.$$

Thus

$$\gamma_p = 2 \quad (d = 3, p_B^Y < p_B < p_B^J).$$

This value for γ_p in three dimensions should also be checked, together with the determination of γ_p in the tetracritical point ($p_B = p_B^J$), by further numerical work.

Acknowledgment

We would like to thank I Kondor, Z Rácz and P Ruján for helpful discussions and comments. This work was partially supported by a contract from the Research Institute for Technical Physics of the Hungarian Academy of Sciences.

Note added in proof. After submitting this paper we received a copy of an article from Professor E K Riedel, in which multicriticality in the Potts model is investigated for general d and q by means of Wilson's exact momentum-space renormalisation-group equation. Newman *et al* (1984) confirm our conjecture $q_m(d) = 2$ ($3 \leq d \leq 4$) by finding that the leading tricritical thermal eigenvalue takes the classical value y_T for all dimensions between three and four in the case $q = 2$.

References

- Andelman D and Berker A N 1981 *J. Phys. A: Math. Gen.* **14** L91
 Baumgärtel H G and Müller-Hartmann E 1982 *Z. Phys. B* **46** 227
 Baxter R J 1973 *J. Phys. C: Solid State Phys.* **6** L445
 Berker A N, Andelman D and Aharony A 1980 *J. Phys. A: Math. Gen.* **13** L413
 Berker A N, Ostlund S and Putnam F A 1978 *Phys. Rev. B* **17** 3650
 Berker A N and Wortis M 1976 *Phys. Rev. B* **14** 4946
 Binder K 1981 *J. Stat. Phys.* **24** 69
 Blankshtein D and Aharony A 1980 *J. Phys. C: Solid State Phys.* **13** 4635
 Blume M 1966 *Phys. Rev.* **141** 517
 Blume M and Watson R E 1967 *J. Appl. Phys.* **38** 991
 Blume M, Emery V J and Griffiths R B 1971 *Phys. Rev. A* **4** 1071
 Burkhardt T W 1976 *Phys. Rev. B* **14** 1196
 ——— 1980 *Z. Phys. B* **39** 159
 Capel H W 1966 *Physica* **32** 966
 Coniglio A 1975 *J. Phys. A: Math. Gen.* **8** 1773
 ——— 1976 *Phys. Rev. B* **13** 2194

- Coniglio A, di Liberto F and Monroy G 1981 *J. Phys. A: Math. Gen.* **14** 3017
- Coniglio A and Klein W 1980 *J. Phys. A: Math. Gen.* **13** 2775
- Coniglio A, Nappi C, Peruggi F and Russo L 1977 *J. Phys. A: Math. Gen.* **10** 205
- Coniglio A, Stanley H E and Klein W 1979 *Phys. Rev. Lett.* **42** 518
- 1982 *Phys. Rev. B* **25** 6805
- den Nijs M P M 1979 *J. Phys. A: Math. Gen.* **12** 1857
- di Liberto F, Monroy G and Palmieri C 1983 *J. Phys. A: Math. Gen.* **16** 405
- Eggarter T P 1974 *Phys. Rev. B* **9** 2989
- Furman D, Dattagupta S and Griffiths R B 1977 *Phys. Rev. B* **15** 441
- Goldschmidt Y Y 1981 *Phys. Rev. B* **24** 1374
- Golner G R 1973 *Phys. Rev. B* **8** 3419
- Griffiths R B 1967 *Physica* **33** 689
- Heermann D W and Stauffer D 1981 *Z. Phys. B* **44** 333
- Kasteleyn P W and Fortuin C M 1969 *J. Phys. Soc. Japan Suppl.* **26** 11
- Kaufman M, Griffiths R B, Yeomans J M and Fisher M E 1981 *Phys. Rev. B* **23** 3448
- Kertész J, Stauffer D and Coniglio A 1982 in *Percolation Structures and Processes* ed G Deutscher, R Zallen and J Adler (Bristol: Adam Hilger)
- Kim D and Joseph R I 1975 *J. Phys. A: Math. Gen.* **8** 891
- Lajzerowicz J and Sivardière J 1975 *Phys. Rev. A* **11** 2079
- Mukamel D and Blume M 1974 *Phys. Rev. A* **10** 610
- Müller-Krumbhaar H 1974 *Phys. Lett.* **50A** 2708
- Newman K E, Riedel E K and Muto S 1984 *Phys. Rev.* **B29** 302
- Nienhuis B 1982 *J. Phys. A: Math. Gen.* **15** 199
- Nienhuis B, Berker A N, Riedel E K and Schick M 1979 *Phys. Rev. Lett.* **43** 737
- Nienhuis B, Riedel E K and Schick M 1980a *J. Phys. A: Math. Gen.* **13** L31
- 1980b *J. Phys. A: Math. Gen.* **13** L189
- 1981 *Phys. Rev. B* **23** 6055
- Pearson R B 1980 *Phys. Rev. B* **22** 2579
- Potts R B 1952 *Proc. Camb. Phil. Soc.* **48** 106
- Rudnick J 1975 *J. Phys. A: Math. Gen.* **8** 1125
- Saul D M, Wortis M and Stauffer D 1974 *Phys. Rev. B* **9** 4964
- Sivardière J and Lajzerowicz J 1975a *Phys. Rev. A* **11** 2090
- 1975b *Phys. Rev. A* **11** 2101
- Stauffer D 1981 *J. Physique Lett.* **42** 99
- Straley J P and Fisher M E 1973 *J. Phys. A: Math. Gen.* **6** 1310
- Sykes M F and Gaunt D S 1976 *J. Phys. A: Math. Gen.* **9** 2131
- Temesvári T and Herényi L 1983 *J. Phys. A: Math. Gen.* **16** L575
- Wang Y K and Wu F Y 1976 *J. Phys. A: Math. Gen.* **9** 593
- Wu F Y 1981 *J. Phys. A: Math. Gen.* **14** L39
- 1982 *Rev. Mod. Phys.* **54** 235
- Yeomans J M and Fisher M E 1981 *Phys. Rev. B* **24** 2825
- Ziman T A L, Amit D J, Grinstein G and Jayaprakash C 1982 *Phys. Rev. B* **25** 319